BUTTERWORTH HEINEMANN

Mixed convection of a micropolar fluid from a rotating cone

Rama Subba Reddy Gorla
Mechanical Engineering University, Cleveland State University, Cleveland, OH

Shoichiro Nakamura
Mechanical Engineering Department, The Ohio State University, Columbus, OH

The nonsimilar boundary-layer solutions are presented to study the mixed convective micropolar fluid flow about a rotating cone. The transformed boundary-layer equations contain an important mixed convection parameter that determines the relative importance of the free convection on forced (rotational) convection. Numerical solutions are presented for a range of values of the material parameters, the buoyancy parameter, and Prandtl number of the fluid. A discussion is provided for the microrotation boundary conditions and their influence on the velocity, gyration, and heat transfer fields.

Keywords: Mixed convection; boundary layers; micropolar fluids; rotating cone

Introduction

There are several practical applications in which significant temperature differences between the surface of the body and the free stream exist. These temperature differences cause density gradients in the fluid medium, and free convection effects become important in the presence of gravitational body force. A situation where both the forced- and free-convection effects are of comparable order is called combined convection. The friction factor and heat transfer rate can be quite different under mixed convection conditions relative to the forced convection case.

Sparrow and Gregg (1959) obtained a similarity solution for the flow of a Newtonian fluid on a rotating disk. The problem of laminar flow of a Newtonian fluid over a rotating cone was studied by We (1959). Hering and Grosh (1963) investigated the effect of free convection on forced convective flow of a rotating cone in a Newtonian fluid. A similrity solution for a rotating cone in a stably stratified medium was given by Himasekhar and Sarma (1986). Lin and Lin (1987) proposed a new similarity variable for the analysis of laminar boundary-layer heat transfer from a rotating cone or disk. Convective heat transfer to non-Newtonian fluids in rotating system is important for thermal design of industrial equipment dealing with such fluids. The mixed convection from a rotating cone to power law fluid has been studied by Wang and Kleinstreuer (1990). Because of the increasing importance in the processing industries and elsewhere of materials whose flow behavior in shear cannot be characterized by Newtonian relationships, a new stage in the evolution of fluid dynamic theory is in progress.

Eringen (1966) formulated the theory of micropolar fluids and derived constitutive laws for fluids with microstructure. This theory included the effects of local rotary inertia and couple stresses and is expected to provide a mathematical model for the non-Newtonian behavior observed in certain manmade liquids such as polymers, colloidal suspensions, fluids with additives, and animal blood. The theory of thermomicropolar fluids with additives, and animal blood. The theory of thermomicropolar fluids has been developed by Eringen (1972) by extending the micropolar fluid theory.

In the present paper, we consider the combined convection from a rotating cone to micropolar fluids with an arbitrary variation of surface temperature. Numerical results are presented for a range of values of the material parameters, the buoyancy parameter, and Prandtl number of the fluid.

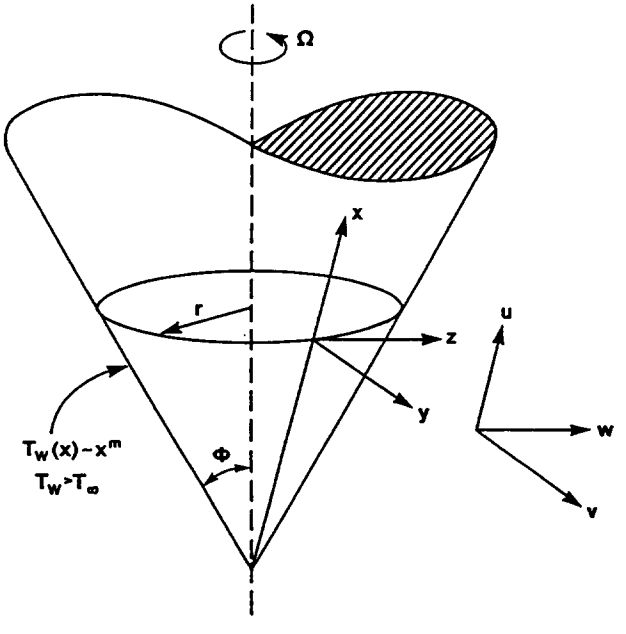

Figure 1 Flow model and coordinate system

Address reprint requests to Professor Gorla at the Mechanical Engineering Dept., Cleveland State University, Cleveland, OH 44115 USA.

Received 28 March 1994; accepted 16 August 1994

Int. J. Heat and Fluid Flow 16: 69–73, 1995

655 Avenue of the Americas, New York, NY 10010

0142-727X/95/$10.00
SSDI 0142-727X(94)00009-2

Analysis

We consider a vertical circular cone rotating about its vertical axis of symmetry in a large body of otherwise quiescent micropolar fluid. The rotational motion of the cone induces a circumferential velocity, and the centrifugal field, thus, impels the fluid along the cone surface. The fluid far from the cone migrates toward it, thus replacing the fluid that has been centrifuged along the cone surface. Figure 1 shows a sketch of the flow model and the coordinate system. It is assumed that the free-stream temperature is constant at T_∞. The surface of the cone is assumed to be $T_w(x)$. It is assumed that viscous dissipation is negligible. Adopting the Boussinesq approxiation, the governing equations may be written within boundary-layer approximation as follows.

Mass:

$$\frac{\partial ru}{\partial x}+\frac{\partial rv}{\partial y}=0 \tag{1}$$

Momentum:

$$u\frac{\partial u}{\partial x}+v\frac{\partial u}{\partial y}-\frac{w^2}{x}=g\beta(T-T_\infty)\cos\phi+\left(\nu+\frac{\kappa}{\rho}\right)\frac{\partial^2 u}{\partial y^2}+\frac{\kappa}{\rho}\frac{\partial N}{\partial y} \tag{2}$$

$$u\frac{\partial w}{\partial x}+v\frac{\partial w}{\partial y}+\frac{uw}{x}=\left(\nu+\frac{\kappa}{\rho}\right)\frac{\partial^2 w}{\partial y^2} \tag{3}$$

Angular momentum:

$$u\frac{\partial N}{\partial x}+v\frac{\partial N}{\partial y}=-\frac{\kappa}{\rho j}\left(2N+\frac{\partial u}{\partial y}\right)+\frac{\gamma}{\rho j}\frac{\partial^2 N}{\partial y^2} \tag{4}$$

Energy:

$$u\frac{\partial T}{\partial x}+v\frac{\partial T}{\partial y}=\alpha\frac{\partial^2 T}{\partial y^2} \tag{5}$$

In the equations above, u, v, and w are the velocity components in the x, y, and z directions, respectively. The component of microrotation is N, and T is the fluid temperature. The appropriate boundary conditions are given by the following:

$$y=0:\ u=0,\ v=0,\ w=r\Omega,\ N=-\frac{1}{2}\frac{\partial u}{\partial y},\ T=T_w(x)$$
$$y\to\infty:\ u\to 0,\ v\to 0,\ w\to 0,\ N\to 0,\ T\to T_\infty \tag{6}$$

The boundary condition for the microrotation assumes that the asymmetric part of the stress tensor vanishes at the surface.

The continuity equation may be satisfied by introducing the stream function ψ defined as follows:

$$ru=\frac{\partial\psi}{\partial y}\quad\text{and}\quad rv=-\frac{\partial\psi}{\partial x} \tag{7}$$

We further define

$$F(\xi,\eta)=\psi/r\alpha\chi,\quad G(\xi,\eta)=w/r\Omega,\quad H(\xi,\eta)=(\alpha^2\chi^3/\nu x^2)^{-1}N,$$
$$\theta=(T-T_\infty)/(T_w-T_\infty),\quad \eta=(y/x)\chi,\quad \xi=\zeta/(1+\zeta),$$
$$\chi=\mathrm{Re}^{1/2}/\xi,\quad \zeta=\mathrm{Re}^{1/2}/\mathrm{Ra}^{1/4},\quad \Delta=\kappa/\mu,$$
$$\lambda=\gamma/\mu j,\quad \mathrm{Re}=x^2\Omega\sin\phi/\nu,\quad \mathrm{Ra}=\frac{g\beta(T_w-T_\infty)x^2\cos\phi}{\alpha\nu},$$
$$(V=(\nu/j\Omega\sin\phi),\quad (T_w-T_\infty)\sim x^m \tag{8}$$

In terms of F, G, H, and q defined in Equation 8, Equations 2–5 are transformed to the following:

$$(1+\Delta)\mathrm{Pr}F'''+\frac{8-(1-\xi)(1-m)}{4}FF''-\frac{2-(1-\xi)(1-m)}{2}(F')^2+\mathrm{Pr}^2\xi^4G^2+\mathrm{Pr}(1-\xi)^4\theta+\Delta H'=\frac{\xi(1-\xi)(1-m)}{4}\left[F'\frac{\partial F'}{\partial\xi}-F''\frac{\partial F}{\partial\xi}\right] \tag{9}$$

$$(1+\Delta)\mathrm{Pr}G''+\frac{8-(1-\xi)(1-m)}{4}FG'-2F'G=\frac{\xi(1-\xi)(1-m)}{4}\left[F'\frac{\partial G}{\partial\xi}-G'\frac{\partial F}{\partial\xi}\right] \tag{10}$$

Notation

F	dimensionless stream function
g	gravitational acceleration
G	dimensionless tangential velocity
h	heat transfer coefficient
H	dimensionless microrotation
j	microinertia per unit mass
L	characteristic length
m	temperature power law index
m_w	couple stress at wall
N	component of microrotation
Nu	Nusselt number
Pr	Prandtl number
r	distance from axis to its surface
Ra	Raleigh number
Re	Reynolds number
T	temperature
U	reference velocity
V	dimensionless material property
u, v, w	velocity components in x, y, and z directions, respectively
x	distance along the cone surface
y	distance normal to the surface
z	tangential coordinate

Greek symbols

α	thermal diffusivity
β	coefficient of thermal expansion
γ	material property of the fluid
η, ξ	dimensionless coordinates
θ	dimensionless temperature
κ	microrotation viscosity parameter
λ, Δ	dimensionless material parameters
ρ	fluid density
τ	shear stress
ϕ	half apex angle of cone
ψ	stream function
Ω	angular velocity

Subscripts

W	surface condition
∞	condition far from the surface

$$\lambda\,\mathrm{Pr}H'' + \frac{8-(1-\xi)(1-m)}{4}FH' + 2HF' - \mathrm{Pr}V\Delta(2H + \mathrm{Pr}F'')\xi^2 = \frac{\xi(1-\xi)(1-m)}{4}\left[F'\frac{\partial H}{\partial \xi} - H'\frac{\partial F}{\partial \xi}\right] \tag{11}$$

$$\theta'' + \frac{8-(1-\xi)(1-m)}{4}F\theta' - mF'\theta = \frac{\xi(1-\xi)(1-m)}{4}\left[F'\frac{\partial \theta}{\partial \xi} - \theta'\frac{\partial F}{\partial \xi}\right] \tag{12}$$

Here, the prime denotes partial differentiation with respect to η alone. The transformed boundary conditions are given by the following:

$$F(\xi,0) = F(\xi,0) = 0, \quad G(\xi,0) = \theta(\xi,0) = 1,$$
$$F(\xi,0) = (\mathrm{Pr}/2)F''(\xi,0), \tag{13}$$
$$F'(\xi,\infty) = \mathrm{G}(\xi,\infty) = \theta(\xi,\infty) = H(\xi,\infty) = 0$$

Equations 9–12 apply to the Newtonian fluid when $\Delta = 0$. The quantity m in the equations above comes from the temperature distribution on the cone surface. The temperature is constant, linear, and parabolic for $m = 0$, 1, and 2, respectively. Equations 9–12 become self-similar when $m = 1$.

The wall shear stress may be written as follows:

$$\tau_w = \left[(\mu + \kappa)\frac{\partial u}{\partial y} + \kappa N\right]_{y=0} \tag{14}$$

The local friction factor is defined as follows:

$$C_{fx} = \tau_w/(\rho U^2/2),$$

where $U = r\Omega + [g\beta(T_w - T_\infty)x]^{1/2}$. Then we can write the following:

$$c_{fx}x/2 = \{(1 + 0.5\Delta)F''(\xi,0)/\mathrm{Pr}\}[\xi^2 + (1-\xi^2)/\sqrt{\mathrm{Pr}}]^{-2} \tag{15}$$

The couple stress at the wall is given by the following:

$$m_w = \gamma\left(\frac{\partial N}{\partial y}\right)_{y=0} = \gamma\left(\frac{\alpha^2\chi^4}{\nu x^3}\right)H'(\xi,0) \tag{16}$$

The Nusselt number Nu_x is given by the following:

$$\mathrm{Nu}_x/\chi = -\theta'(\xi,0) \tag{17}$$

The numerical scheme to solve Equations 9–13 adopted here is based on the finite difference of scheme developed by Gorla et al. (1993). These details are not reproduced here to conserve space.

The numerical results are affected by the number of mesh points in both directions. To obtain accurate results, a mesh sensitivity study was performed. In the η direction, after the results for the mesh points of 51, 100, 190, 800 were compared, it was found that 190 points give the same results as 800. In the x direction, only 11 mesh points were found to give as accurate results as with 21 points. Therefore, the remainder of the computations were performed with 190 times 11 mesh points. If the numerical scheme written in this section is used for Pr that substantially deviates from 1, particularly for a much smaller Pr, both η_{max} and the mesh sizes must be reoptimized.

To examine the validity and accuracy of the present scheme, we compare our results with the published data for the Newtonian fluid cases. For comparison with the literature data, we consider the forced convection with the constant temperature on the cone surface. for Pr = 1 and 10, our results agree well with those of Wang and Kleinstreuer (1990), as shown in Table 1. Comparison for other Pr numbers are not shown, because the mesh size and η_{max} have been optimized for Pr = 10.

Table 1 Comparison of $\theta^{*\prime}$ (0) to Wang and Kleinstreuer (1990)*

	Pr = 1	Pr = 10
Wang and Kleinstreuer	0.62894	0.56066
Present work	0.62853	0.56087

* $-\theta^{*\prime}(0) = -\theta'(0)(1 + \mathrm{Pr})^{2/3}/\mathrm{Pr}$

Results and discussion

Figures 2–5 display the profiles of axial velocity, tangential velocity, microrotation, and temperature within the boundary layer for the linear surface temperature case. The evolution of the axial velocity profile $F'(\eta, \xi)$ from the pure free convection ($\xi = 0$) to pure forced convection ($\xi = 1$) is seen in Figure 2. Initially as ξ increases, the peak axial velocity decreases with diminishing free-convection effect. However, for $\xi \geq 0.6$, the amplitude of F' increases with increasing rotation of the cone, thus indicating a change in momentum transport mechanism.

Figure 3 illustrates that the dimensionless radial velocity profile broadens initially as ξ increases and then tends to

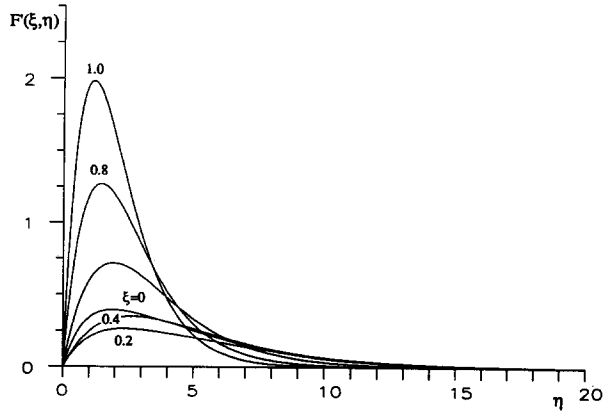

Figure 2 Axial velocity profiles

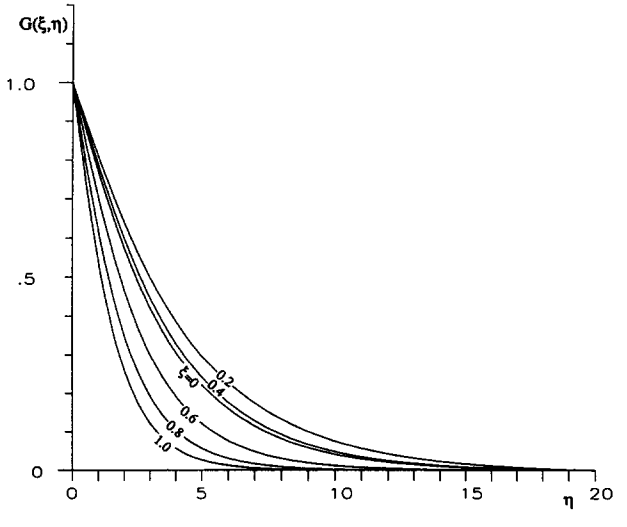

Figure 3 Radial velocity profiles

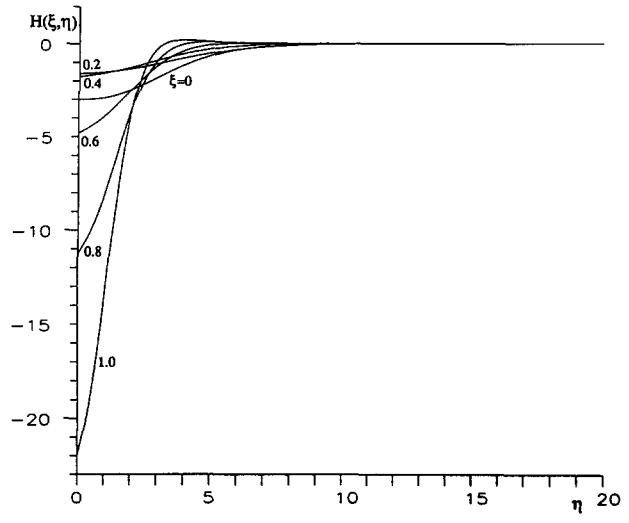

Figure 4 Microrotation profiles

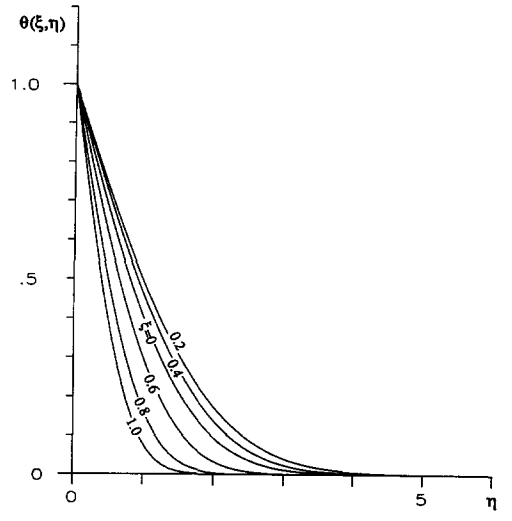

Figure 5 Temperature profiles

become shallower for $\xi \geq 0.6$. Figure 4 illustrates the microrotation profiles. We observe that as ξ increases, initially the microrotation profiles tend to become flatter, and then for $\xi \geq 0.6$, the microrotation profiles have a high positive gradient at the wall. From Figure 5, we observe that the temperature distribution within the boundary layer initially broadens with ξ and then, for $\xi > 0.6$, the temperature profiles become shallower.

In the free-convection regime, the heat transfer rate decreases with increasing values of ξ, and then increases with increasing values of ξ in the forced convection regime, where the transport phenomenon is dominated by the rotational motion of the cone. The heat transfer rate increases as m increases. This behavior is displayed in Figure 6.

Table 2 summarizes our numerical results for $F''(\xi, 0)$, $G'(\xi, 0)$, $H'(\xi, 0)$, and $\theta'(\xi, 0)$ with Δ and λ treated as prescribed

Table 2 Computed results of F', G', H' and θ' at the wall for $m = 1$ (Pr = 10, $V = 0.1$)

ξ	λ	Δ	$F'(\xi, 0)$	$G'(\xi, 0)$	$H'(\xi, 0)$	$\theta'(\xi, 0)$
0.0	0.5	0.5	0.60072	−0.24239	−0.00209	−0.57719
0.0	0.5	5.0	0.24662	−0.11594	−0.00032	−0.52407
0.0	0.5	50.0	0.04908	−0.06830	0.00339	−0.30353
0.0	5.0	0.5	0.59244	−0.23904	0.12469	−0.66965
0.0	5.0	5.0	0.23413	−0.11165	0.05385	−0.50606
0.0	5.0	50.0	0.04889	−0.06817	0.01467	−0.29934
0.2	0.5	0.5	0.32173	−0.19811	0.05311	−0.55081
0.2	0.5	5.0	0.14573	−0.09809	0.13554	−0.43654
0.2	0.5	50.0	0.03482	−0.06752	0.05370	−0.26225
0.2	5.0	0.5	0.31726	−0.19573	0.08407	−0.54526
0.2	5.0	5.0	0.13051	−0.09691	0.05535	−0.41808
0.2	5.0	50.0	0.03090	−0.06751	0.02878	−0.25518
0.4	0.5	0.5	0.35640	−0.22111	0.17707	−0.59012
0.4	0.5	5.0	0.21050	−0.11619	0.27386	−0.51591
0.4	0.5	50.0	0.04512	−0.06826	0.06272	−0.30123
0.4	5.0	0.5	0.34677	−0.21894	0.10436	−0.58255
0.4	5.0	5.0	0.18379	−0.11512	0.12352	−0.49335
0.4	5.0	50.0	0.04275	−0.06822	0.04751	−0.29724
0.6	0.5	0.5	0.96416	−0.31483	0.73236	−0.83249
0.6	0.5	5.0	0.63702	−0.16756	1.07474	−0.75813
0.6	0.5	50.0	0.17441	−0.07395	0.22513	−0.49607
0.6	5.0	0.5	0.93042	−0.31157	0.30296	−0.81963
0.6	5.0	5.0	0.55990	−0.16721	0.52956	−0.72701
0.6	5.0	50.0	0.16951	−0.07385	0.19577	−0.49205
0.8	0.5	0.5	2.25996	−0.41907	2.27928	−1.10896
0.8	0.5	5.0	1.51413	−0.22316	3.33097	−1.01498
0.8	0.5	50.0	0.49281	−0.08550	0.68984	−0.71179
0.8	5.0	0.5	2.17598	−0.41462	0.82252	−1.09085
0.8	5.0	5.0	1.33247	−0.22315	1.66395	−0.97354
0.8	5.0	50.0	0.48429	−0.08545	0.62312	−0.70835
1.0	0.5	0.5	4.40723	−0.52421	5.52277	−1.38938
1.0	0.5	5.0	2.96261	−0.27903	8.09658	−1.27242
1.0	0.5	50.0	1.05144	−0.10110	1.66061	−0.92232
1.0	5.0	0.5	4.24078	−0.51858	1.90867	−1.36628
1.0	5.0	5.0	2.60702	−0.27904	4.06009	−1.22019
1.0	5.0	50.0	1.03744	−0.10116	1.52246	−0.91894

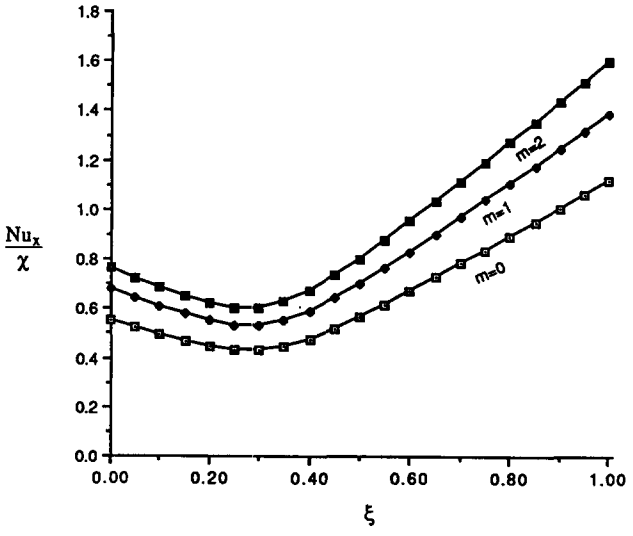

Figure 6 Nusselt number *versus* ξ

parameters. This information is useful in the evaluation of wall shear stress, wall couple stress, and heat transfer rate, as described by Equations 14–17. Table 3 shows a comparison of the results for the case of Newtonian fluids. A comparison of the results in Tables 2 and 3 indicates that micropolar fluids exhibit reduction in drag as well as heat transfer rate. For example, when $\xi = 0$, $\lambda = 0.5$ and $\Delta = 0.5$, 5 and 50, we notice that the ratio of friction factor for the micropolar to Newtonian fluids is 0.7816, 0.3209, and 0.0639 respectively. Similarly, the ratio of heat transfer rates for the above combination of material parameters for the micropolar to Newtonian fluids is 0.9423, 0.7292, and 0.4223, respectively. This suggests that the micropolar fluids may be useful in several practical applications.

Concluding remarks

In this paper we used the theory of micropolar fluids formulated by Eringen (1966) to derive a set of boundary-layer equations for the combined convection from a rotating cone. Numerical solutions are presented for the fluid flow and heat transfer characteristics, and their dependence on the pertinent material parameters is discussed. The wall values of the velocity, microrotation, and temperature are tabulated for a wide range of the dimensionless grouping of material parameters. This information would be useful to evaluate the surface friction factor and wall couple stress, as well as the heat transfer rate. The numerical results indicate that the micropolar fluids display a reduction in drag as well as surface heat transfer rate when compared to the Newtonian fluid.

Table 3 Computed results of F', G', H', and θ' at the wall for Newtonian fluid (Pr = 10)

	ξ	$F(\xi, 0)$	$G'(\xi, 0)$	$\theta'(\xi, 0)$
$m = 1$	0.000	0.76862	−0.29446	−0.71867
	0.200	0.40842	−0.24072	−0.58307
	0.400	0.42263	−0.26276	−0.60839
	0.600	1.11318	−0.37107	−0.85027
	0.800	2.60397	−0.49382	−1.13219
	1.000	5.07494	−0.61792	−1.41874

Acknowledgments

The computations were done on the computer for facilities of NASA Lewis Research Center. The authors are grateful for the assistance of E. S. Reddy of Sverdrup Corporation in the use of the computers. The authors thank the referees for their useful comments. The present work was performed at Ohio Aerospace Institute.

References

Eringen, A. C. 1966. Theory of micropolar fluids. *J. Math. Mech.*, **16**, 1

Eringen, A. C. 1972. Theory of thermomicrofluids. *J. Math. Anal. Appl.*, **38**, 480

Gorla, R. S. R., Lee, J. K., Nakamura, S. and Pop, I. 1993. Effects of transverse magnetic field on mixed convection in wall plume of power-law fluids. *Int. J. Eng. Sci.*, **31**, 1035–1045

Hering, R. G. and Grosh, R. J. 1963. Laminar combined convection from a rotating cone. *J. Heat Transfer*, **85**, 29

Himasekhar, K. and Sarma, P. K. 1986. Laminar combined convection from a rotating cone to a thermally stratified environment. *J. Heat Transfer*, **108**, 973

Lin, H. T. and Lin, L. K. 1987. Heat transfer from a rotating cone or disk to fluids of any Prandtl number. *Int. Comm. Heat Mass Transfer*, **14**, 323

Sparrow, E. M. and Gregg, J. L. 1959. Heat transfer from a rotating disk to fluids of any Prandtl number. *J. Heat Transfer*, **81**, 249

Wang, T. Y. and Kleinstreuer, C. 1990. Similarity solutions of combined convection heat transfer from a rotating cone or disk to non-Newtonian fluids. *J. Heat Transfer*, **112**, 939

Wu, C. 1959. The three-dimensional incompressible laminar boundary layer on a spinning cone. *Appl. Sci. Res.*, **8**, 140